ELECTRONIC SUPPORTING INFORMATION FOR

Supported nickel-rhenium catalysts for selective hydrogenation of methyl esters to alcohols

Kaituo Liu[a,‡], James Pritchard[a,‡], Li Lu[b], Robbert van Putten[a], M.W.G.M. (Tiny) Verhoeven[a], Mike Schmitkamp[c], Xiaoming Huang[a], Laurent Lefort[c], Christopher J. Kiely[b], Emiel J. M. Hensen[a*], Evgeny A. Pidko[a,d*]

[a] *Inorganic Materials Chemistry group, Schuit Institute of Catalysis, Eindhoven University of Technology, P.O. Box 513, 5600 MB Eindhoven, the Netherlands*

[b] *Department of Materials Science and Engineering, Lehigh University, 5 East Packer Avenue, Bethlehem, PA 18015, U.S.A.*

[c] *DSM Innovative Sciences, Synthesis BV, P.O. Box 18, 6160 MD Geleen, The Netherlands.*

[d] *ITMO University, Lomonosova str. 9, St. Petersburg 191002, Russia*

* Corresponding authors:

Emiel J.M. Hensen, Tel: +31 40 247 51 78, e-mail: e.j.m.hensen@tue.nl

Evgeny A. Pidko, Tel: +31-40-247-2189, e-mail: e.a.pidko@tue.nl

Contents

S1. Experimental detals

S1.1. Catalyst Preparation

Catalysts precursors, reactants and solvents were obtained from Sigma Aldrich: perrhenic acid, $HReO_4$ (75 wt.%, aqueous), nickel nitrate hexahydrate, $Ni(NO_3)_2 \cdot 6H_2O$, methyl hexanoate (99.9%), ethyl hexanoate (99.9%), methyl benzoate (99.9%), hexanoic acid (99.9%) and hexane (99%) were used as received without additional purification. Catalyst supports were obtained from the following sources: α-Al_2O_3 (Condea), Carbon (RX-3, Norit), CeO_2 (Sigma Aldrich), SiO_2 (Grace), TiO_2 (P-25, Degussa). Supported 3 wt% Ni-*x* wt% Re catalysts were synthesized by wet-impregnation with all quantities listed per gram of catalyst. Re contents in the prepared catalysts were:

Ni:Re molar ratio	(5:1)	(5:2)	(2:1)	(1:1)	(1:2)	(1:4)
wt.% Re	1.9	3.8	4.8	9.5	19	38.1

In a typical procedure, $HReO_4$ (34-169 µL) was added to a solution of $Ni(NO_3)_2 \cdot 6H_2O$ (0.1486 g). The appropriate amount of support (125-250 µm) was then added to the solution while stirring at 80 °C. The material was dried (110 °C, 16 h), ground using a pestle and mortar and reduced at 300 °C in 10% H_2/He (100 ml/min) for 2 h.

S1.2. Catalyst characterisation

S1.2.1. Transmission electron microscopy (TEM)

Transmission electron micrographs were acquired on a FEI Tecnai 20 transmission electron microscope at an acceleration voltage of 200 kV with a LaB_6 source. Typically, a small amount of the sample was ground and suspended in pure ethanol, sonicated and dispersed over a Cu grid with a holey carbon film. Samples were first reduced in 10 vol.% H_2 in He (total flow 100 mL min^{-1}) at 300 °C for 2 hours, followed by passivation in 1 vol.% O_2 in He for 2 h. Materials for analysis by scanning transmission electron microscopy (STEM) were dry dispersed onto a holey carbon TEM grid. The catalyst samples were examined using high angle annular dark field (HAADF) imaging mode in an aberration corrected JEOL ARM-200CF TEM/STEM operating at 200 kV. This microscope was also equipped with a Centurio silicon drift detector (SDD) system for X-ray energy dispersive spectroscopy (XEDS) analysis.

S1.2.2. X-ray Energy Dispersive Spectroscopy (XEDS).

Quantification of the XEDS spectra was carried out via the Thermo NORAN System SIX (NSS) software using the Cliff-Lorimer method assuming no X-ray absorption.[S1]The Ni Kα (peak range: 7331-7623 eV) and Re Lα (peak range: 8496-8806 eV) were used to quantify the relative proportions of the two elements in the areas analyzed. Standardless Gaussian fitting was applied to the two characteristic peaks, with the k-factors pre-determined by the NSS software ($k_{Ni\ K\alpha}$=1.217, $k_{Re\ L\alpha}$=2.652)

[S1] G. Cliff and G. Lorimer, the quantitative analysis of thin specimens. [*J. Microsc.* 1975, **103**, 203.]

S1.2.3. Temperature-programmed reduction (TPR)

H_2-TPR experiments were performed in a Micromeritics Autochem II 2920 equipped with a fixed-bed reactor, a computer-controlled oven, and a thermal conductivity detector. Typically, 50 mg catalyst was loaded in a tubular quartz reactor. The sample was reduced in 4 vol.% H_2 in N_2 at a flow rate of 10 mL/min, while heating from room temperature up to 700 °C at a ramp rate of 2 °C/min. The H_2 signal was calibrated using a CuO/SiO_2 reference catalyst.

S1.2.4. X-ray photoelectron spectroscopy (XPS)

XPS measurements were carried out with a Thermo Scientific K-Alpha, equipped with a monochromatic small-spot X-ray source and a 180° double focusing hemispherical analyzer with a 128-channel detector. Spectra were obtained using an aluminium anode (Al K_α = 1486.6 eV) operating at 72 W and a spot size of 400 µm. Survey scans were measured at a constant pass energy of 200 eV and region scans at 50 eV. The background pressure was 2×10^{-9} mbar and during measurement 3×10^{-7} mbar Ar because of the charge compensation by the dual-beam low energy electron / Arion source. Data analysis was performed using CasaXPS software. The binding energy was corrected for surface charging by taking the C 1s peak of adventitious carbon as a reference at 284.6 eV.

S1.3 Catalyst activity measurements

All hydrogenation experiments were prepared inside a large, two-hand glove bag (AtmosBag with zipper lock, Sigma Aldrich). The glove bag was purged five times with nitrogen after which a constant flow rate was applied to give a suitable working over-pressure. A pre-reduced catalyst (3–18 mg) was then loaded into a small stainless steel autoclave followed by the addition of solvent (3.5 mL), substrate (0.44 mmol) and internal standard (dodecane, 35.2 µL) after which the autoclave was sealed and removed from the glove bag. The catalytic reactions were carried in the absence of any source of light. The autoclave was subsequently purged five times with hydrogen (2 MPa) before filling the vessel to the desired pressure (5 MPa). Using a hot plate equipped with magnetic stirring capability, the autoclave was gradually heated to 180 °C (unless otherwise stated) before stirring at 1000 rpm was commenced (1-8 h). On completion of the reaction, both heating and stirring were stopped, the autoclave was removed from the hot plate and then cooled in ice-cold water. Once cooled, the contents of the autoclave were filtered using an organic-based polymer frit and a sample was prepared for GC-FID analysis (Shimadzu GC-FID equipped with RX-5 carbowax column). Calibration was performed using known concentrations of all reactants and products in order to determine correct response factors.

S2. Supplementary results

S2.1. Catalytic activity testings

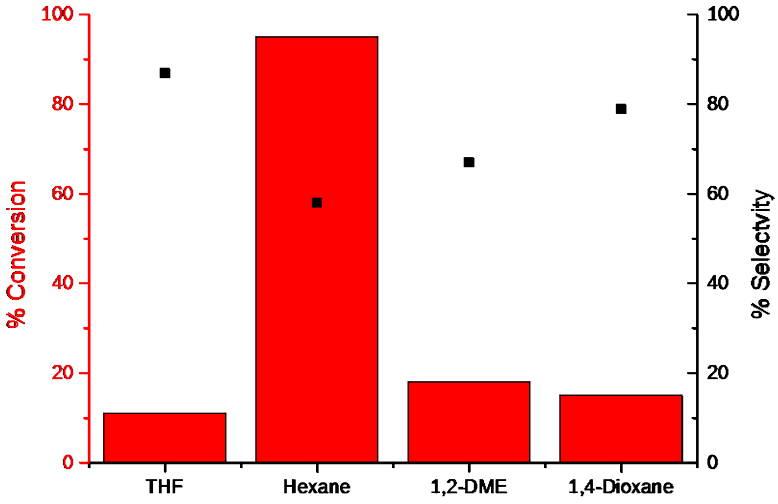

Figure S1 Effect of solvent on the performance of Ni-Re (1:2)/TiO_2 catalysts in the hydrogenation of methyl hexanoate. *Conditions:* Catalyst (18 mg), methyl hexanoate (0.44 mmol), hexane (3.5 mL), dodecane (35.2 µL), 180 °C, 50 bar H_2, 8 h, 1000 rpm.

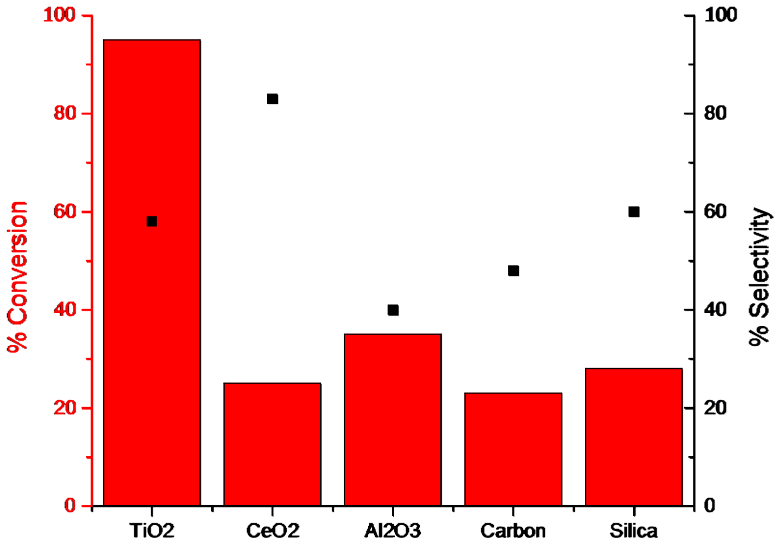

Figure S2 Effect of catalyst support on the performance of Ni-Re (1:2) catalysts in the hydrogenation of methyl hexanoate. *Conditions:* Catalyst (18 mg), methyl hexanoate (0.44 mmol), hexane (3.5 mL), dodecane (35.2 µL), 180 °C, 50 bar H_2, 8 h, 1000 rpm.

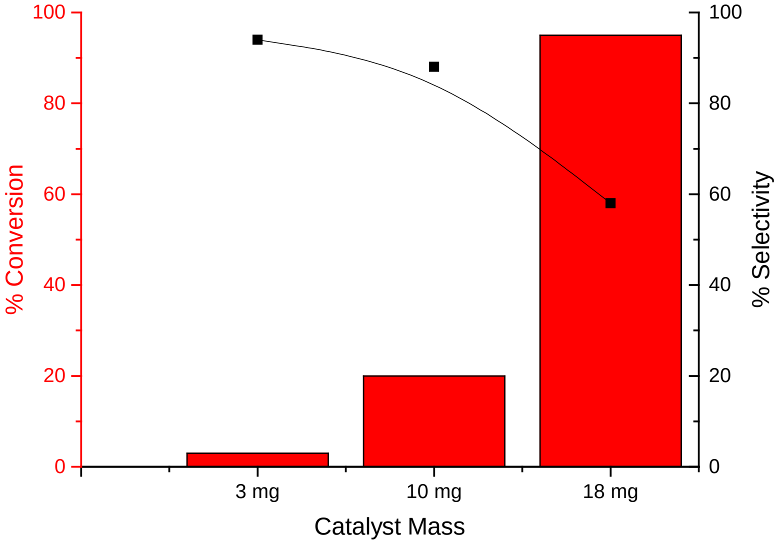

Figure S3 Effect of catalyst loading on the performance of Ni-Re (1:2)/TiO_2 catalysts in the hydrogenation of methyl hexanoate. *Conditions:* Catalyst (3-18 mg), methyl hexanoate (0.44 mmol), hexane (3.5 mL), dodecane (35.2 µL), 180 °C, 50 bar H_2, 8 h, 1000 rpm.

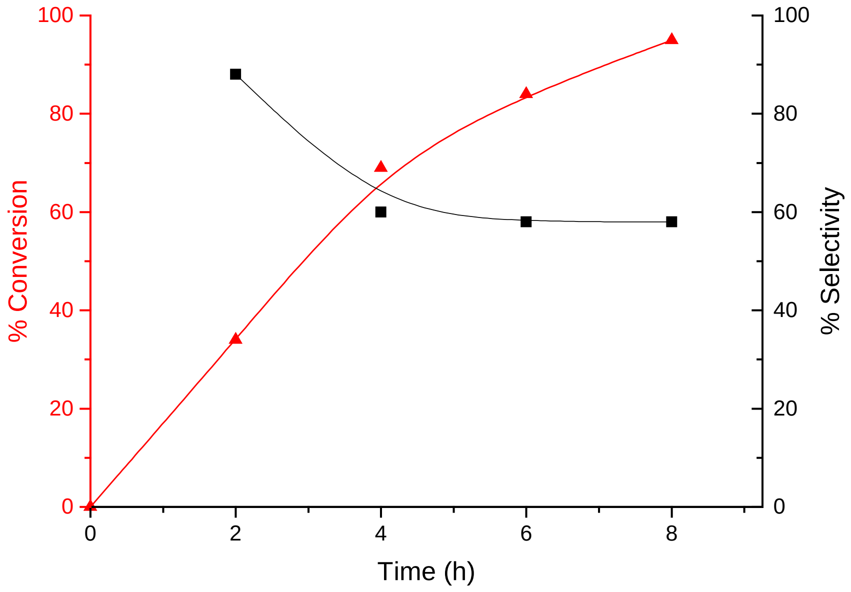

Figure S4 Time-on-line analysis of the conversion of methyl hexanoate in hexane solvent and its selectivity to hexanol for Ni-Re (1:2)/TiO_2 catalysts. *Conditions:* Catalyst (18 mg), methyl hexanoate (0.44 mmol), hexane (3.5 mL), dodecane (35.2 µL), 180 °C, 50 bar H_2, 2-8 h, 1000 rpm.

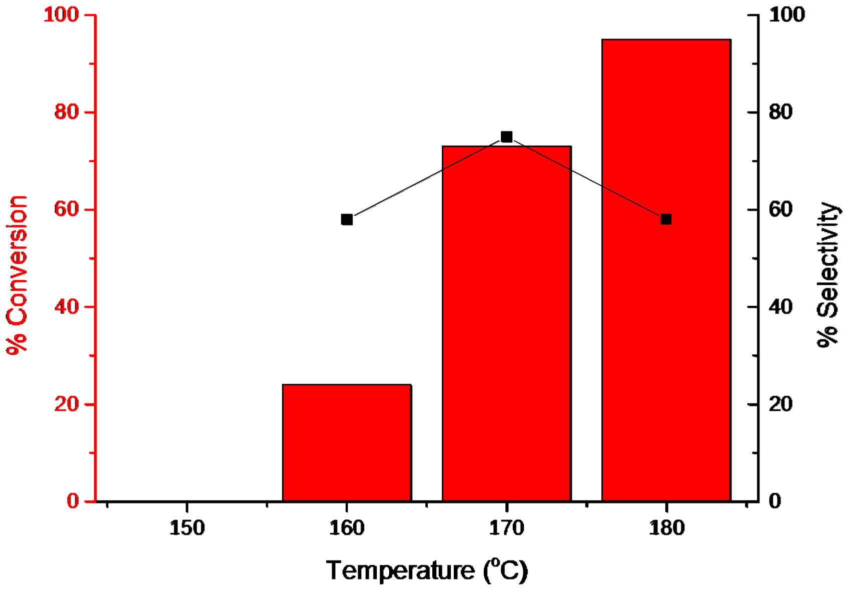

Figure S5 Effect of reaction temperature on the performance of Ni-Re (1:2)/TiO_2 catalysts in the hydrogenation of methyl hexanoate. *Conditions:* Catalyst (18 mg), methyl hexanoate (0.44 mmol), hexane (3.5 mL), dodecane (35.2 µL), 180 °C, 50 bar H_2, 8 h, 1000 rpm.

S2.2. STEM-HAADF characterisation

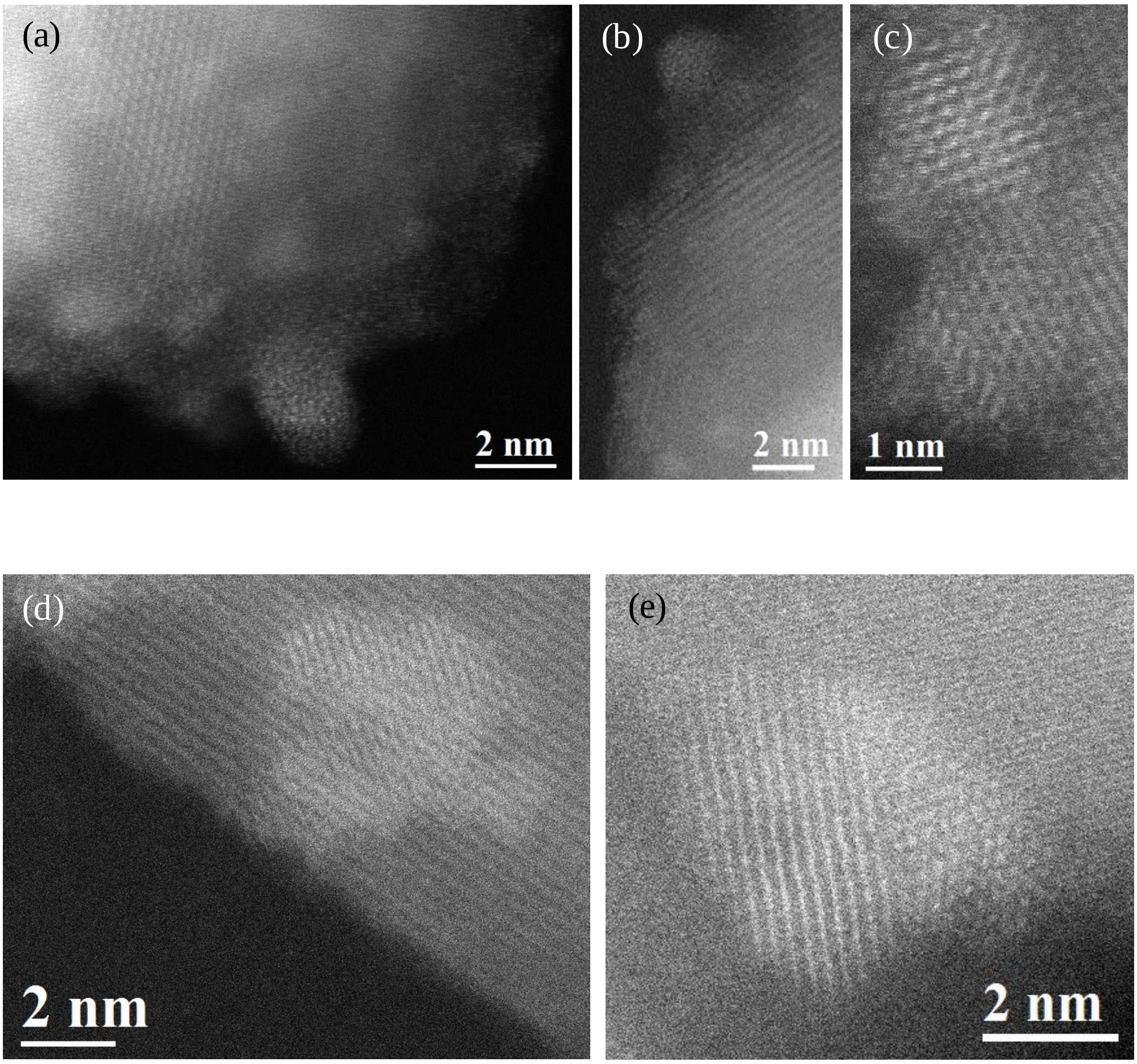

Figure S6 Representative STEM-HAADF micrographs of the Ni /TiO_2 catalyst. (a) shows a lower magnification view in which 2-3 nm Ni containing particles are primarily visible similar to the BF-TEM images presented in Figure 2. Some of the particles appear disordered in nature (a,b) while others are clearly more crystalline (c, d, e). More detailed analysis of the lattice fringe spacings and intersection angles suggest the latter are primarily NiO. These Ni-containing particles exhibit relatively low contrast in these HAADF images due to the similarity in atomic number between Ti (z = 22) and Ni (z = 28). The much stronger contrast shown by Re atoms in the subsequent HAADF images presented in Figures S7 and S8 is due to the significantly higher mass of Re (z = 75).

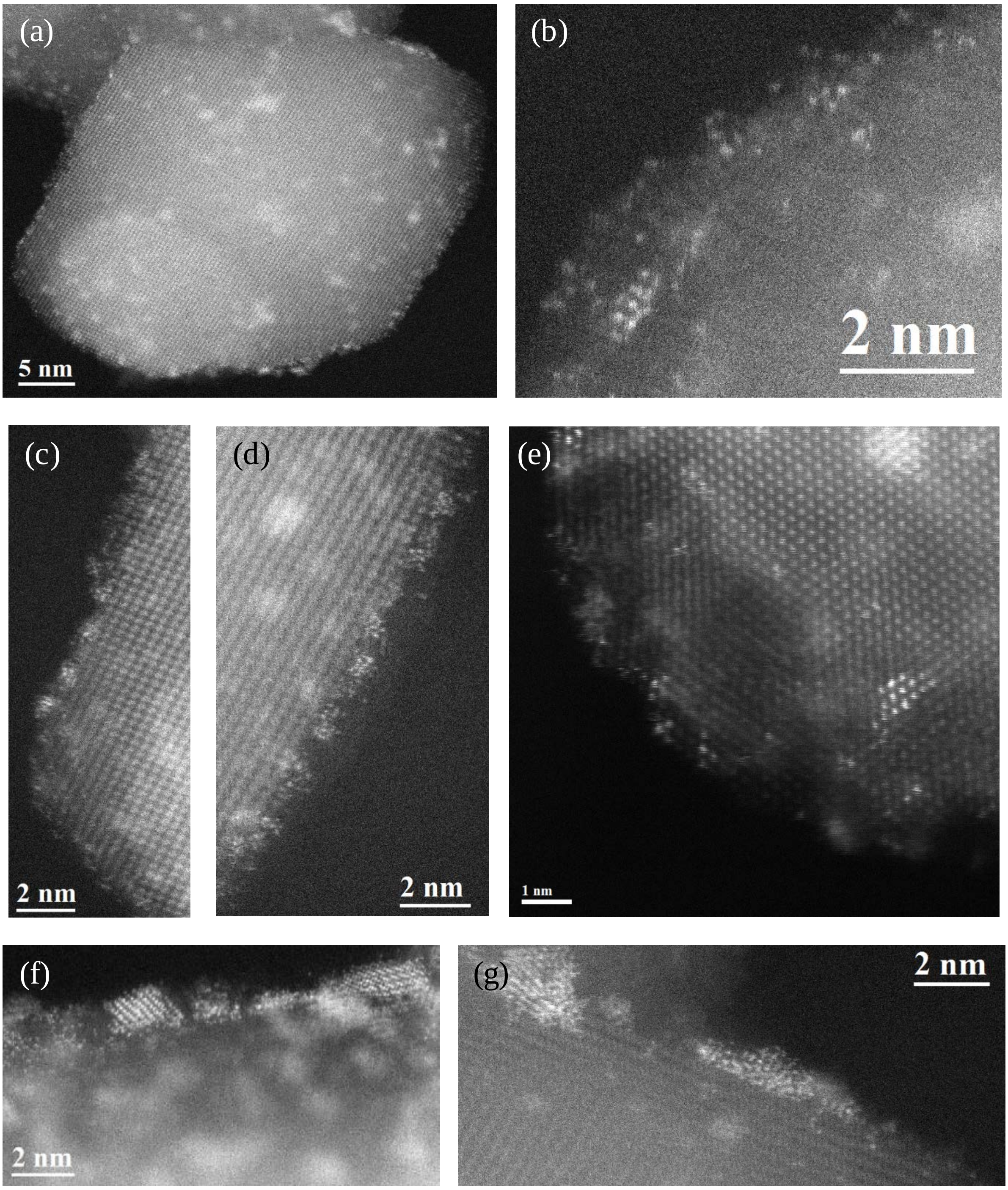

Figure S7 Representative STEM-HAADF micrographs of the Ni-Re (1:2)/TiO_2 catalyst. (a) shows a lower magnification view in which 1-2 nm Ni-Re containing particles are primarily visible similar to the BF-TEM images presented in Figure 2. Higher magnification micrographs show the additional co-existence of (b) atomically dispersed Re and Ni species, (c, d) disordered sub-nm Re and Ni containing clusters, (e) ordered epitaxial Re-containing rafts, (f) crystalline Ni-Re metallic nanoparticles and (g) more extended disordered Ni- and Re- containing surface films.

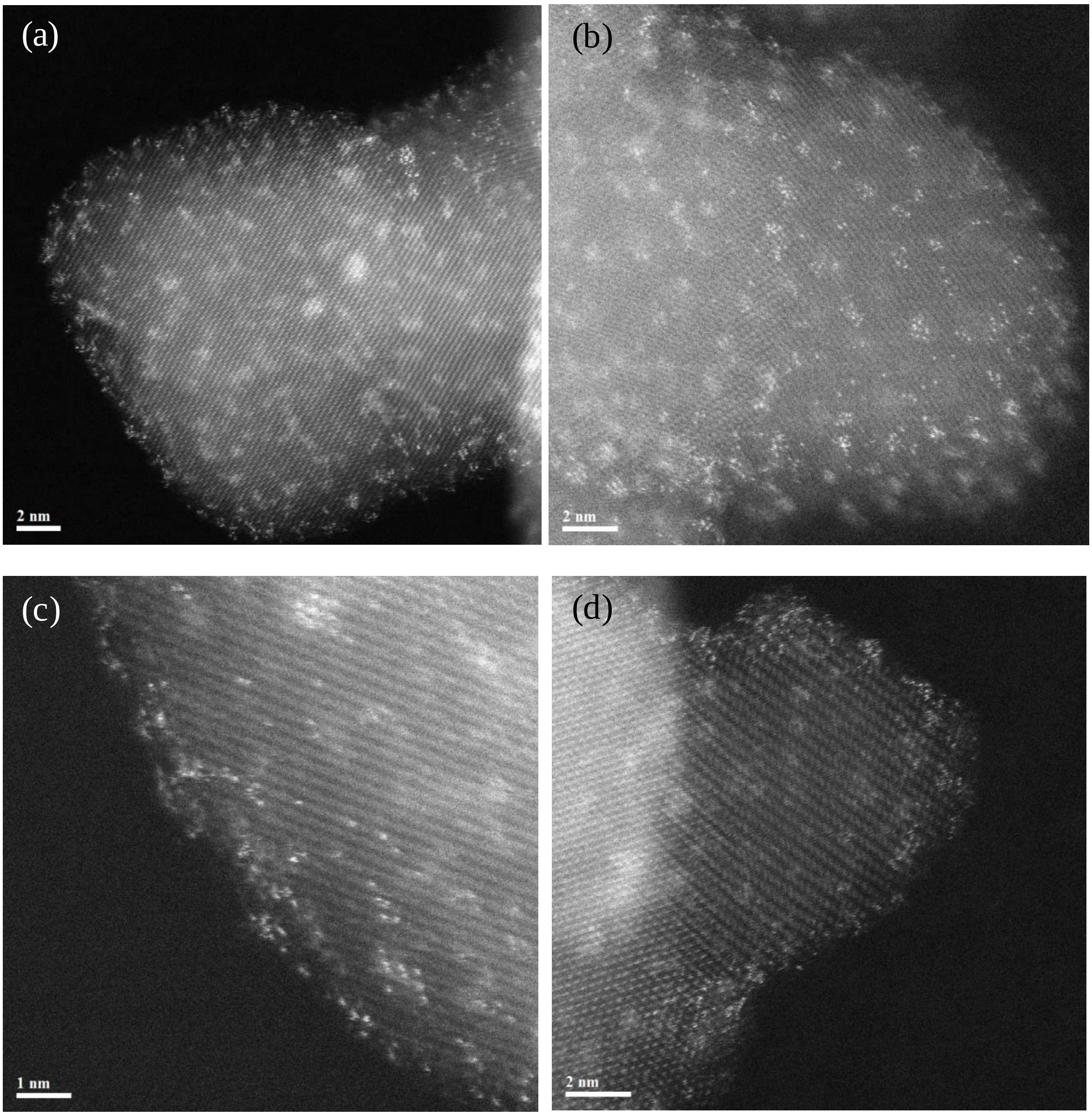

Figure S8 Representative STEM-HAADF micrographs of the Ni-Re (5:2)/TiO_2 catalyst. (a) shows a lower magnification view in which ~1 nm Ni-Re containing particles are primarily visible similar to the BF-TEM images presented in Figure 2. Higher magnification images show a proliferation of sub-nm mixed Ni-Re clusters and atomically dispersed species in this sample. Noticeably fewer particles in the 1-2 nm size range were found in this lower Re content sample as compared to the Ni-Re (1:2)/TiO_2 catalyst shown in Figure S7.

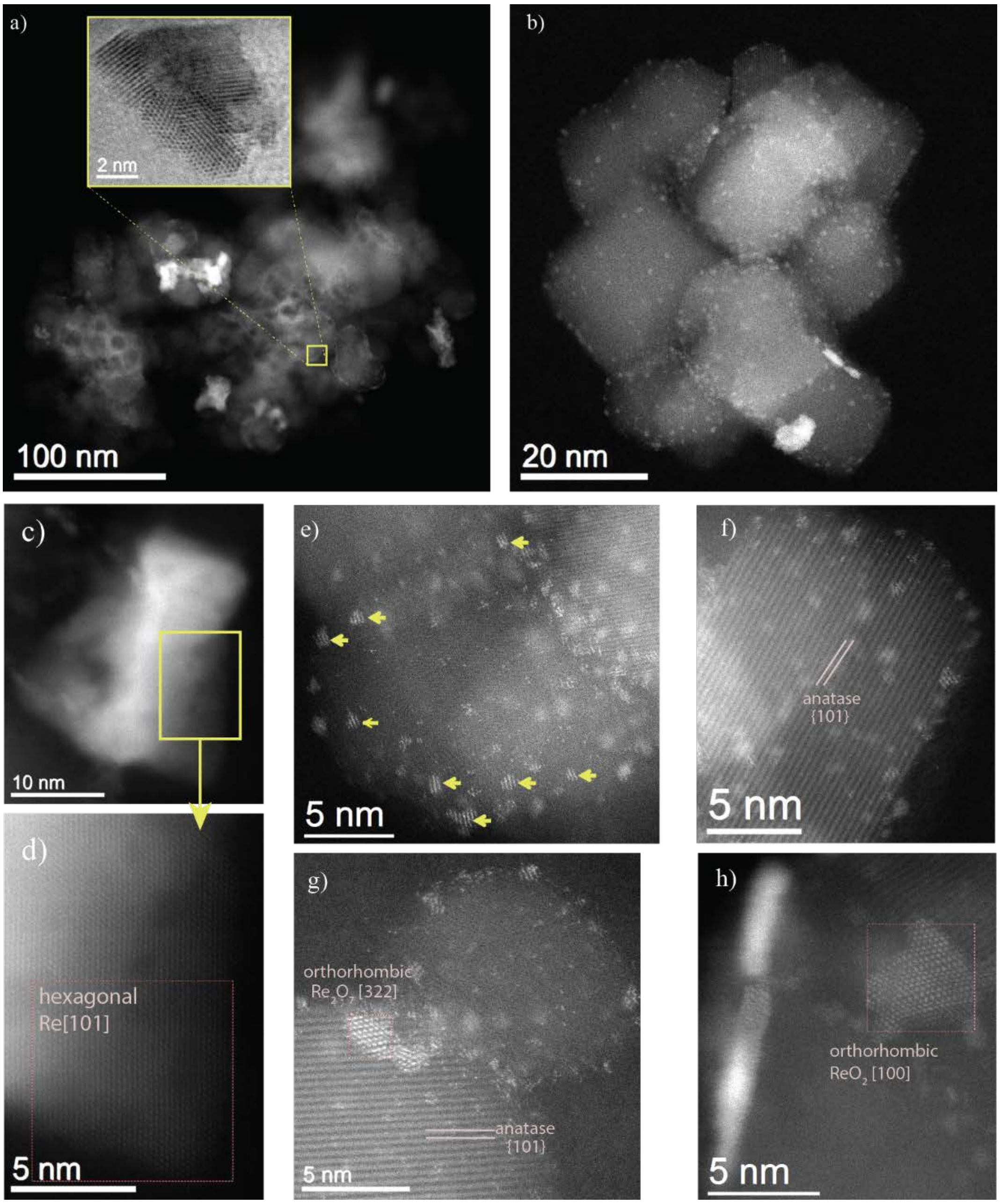

Figure S9. Representative STEM-HAADF micrographs of the Re (18 wt. %)/TiO$_2$ catalyst. (a) and (b) show lower magnification views evidencing inhomogeneous distributions Re-containing nanoparticles (NPs). Although some very larger aggregates can be noted in (a), smaller polycrystalline aggregates of <10 nm (inset in (a)) are more populous. Lattice fittings of large NPs suggest that they are metallic Re (c,d). Higher magnification images evidence the presence of NPs of different size including nanocrystals (e-h), clusters and Re atoms (e,f,h). Lattice fringes of ~ 1nm nanocrystals (yellow arrows) in (e) appear to be parallel to each other, suggesting their epitaxial relation with the support. The crystalline NPs in (g) and (h) were fitted to Re$_2$O$_7$ and ReO$_2$, respectively. The collected data indicates the presence of crystalline NPs with Re in different oxidation states, with more oxidized Re observed in smaller NPs.

S2.3. X-ray Energy Dispersive Spectroscopy

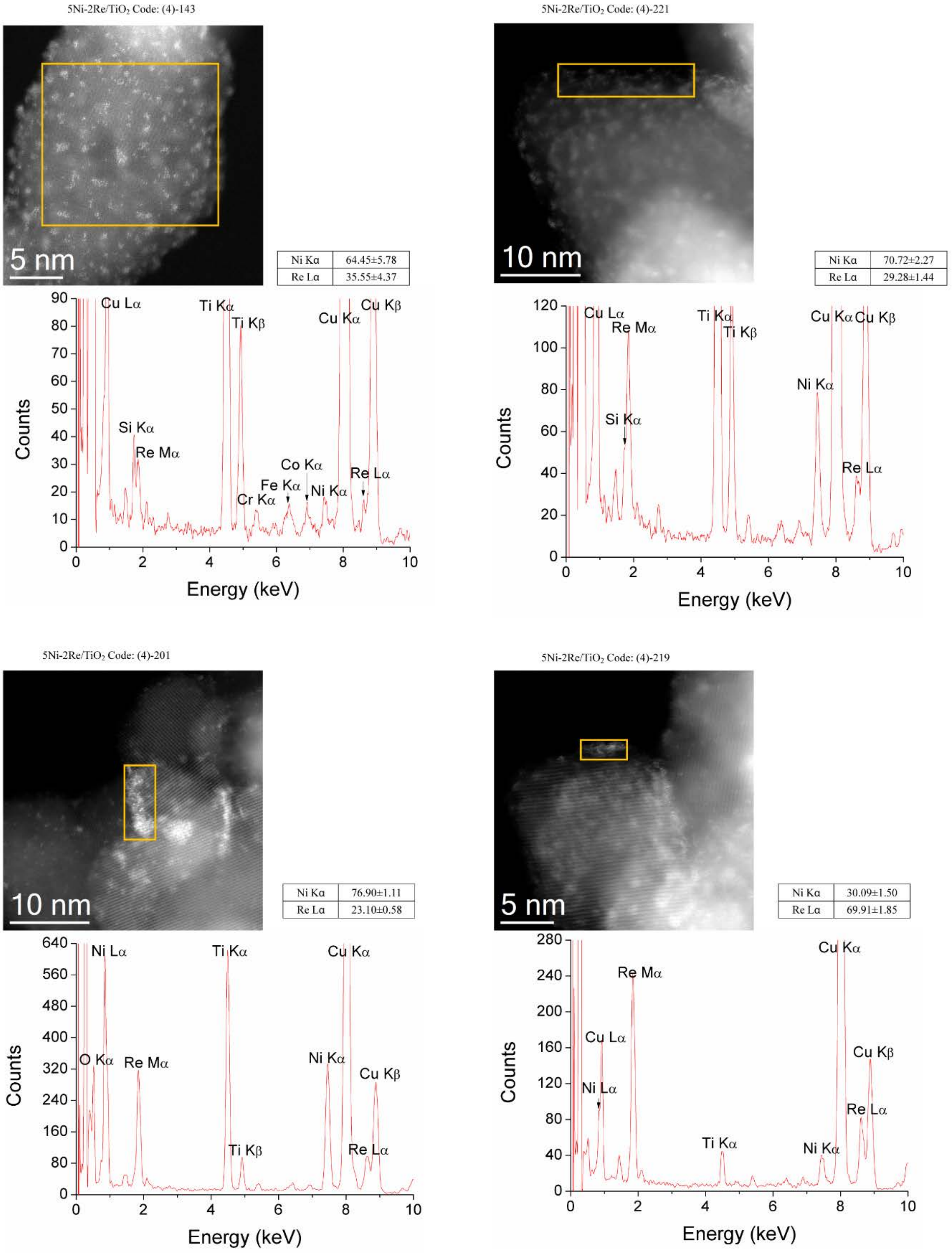

5Ni-2Re/TiO₂ Code: (4)-143

Ni Kα	64.45±5.78
Re Lα	35.55±4.37

5Ni-2Re/TiO₂ Code: (4)-221

Ni Kα	70.72±2.27
Re Lα	29.28±1.44

5Ni-2Re/TiO₂ Code: (4)-201

Ni Kα	76.90±1.11
Re Lα	23.10±0.58

5Ni-2Re/TiO₂ Code: (4)-219

Ni Kα	30.09±1.50
Re Lα	69.91±1.85

Figure S10. Representative STEM-HAADF micrographs together with the respective XEDS spectra and the results of their quantification for Ni-Re (5:2)/TiO_2 catalyst evidencing the formation of bimetallic nanoparticles and clusters.

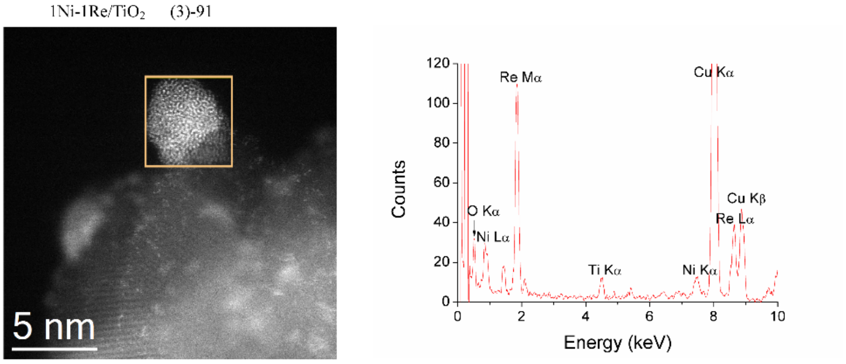

Ni Kα	22.58±2.01
Re Lα	77.42±3.02

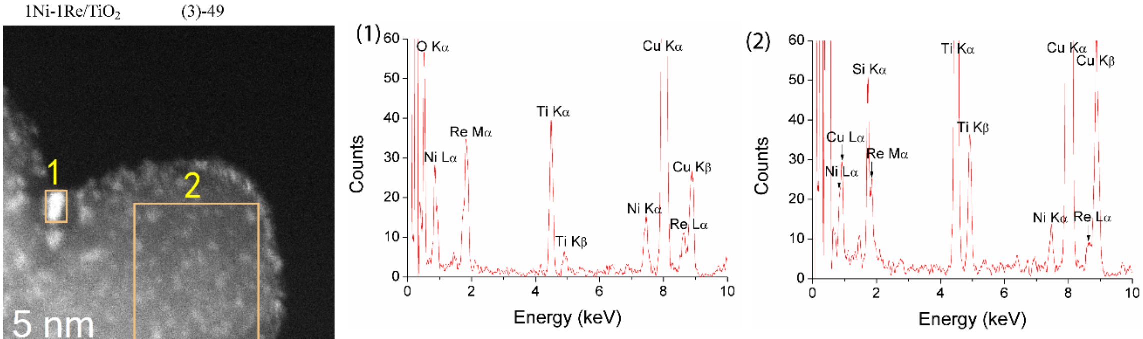

Atom%	Box 1	Box 2
Ni Kα	59.67±5.16	63.69±6.78
Re Lα	40.33±3.99	36.31±5.28

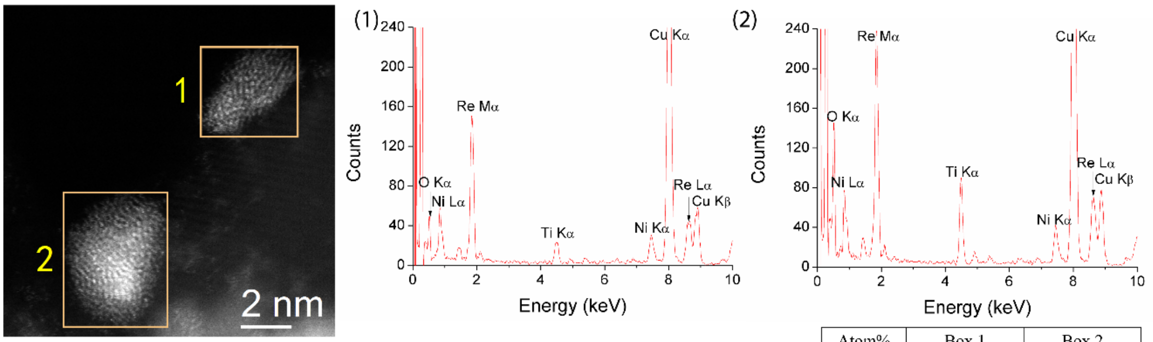

Atom%	Box 1	Box 2
Ni Kα	33.53±1.85	29.94±1.45
Re Lα	66.47±2.12	70.06±1.78

Figure S11. Representative STEM-HAADF micrographs together with the respective XEDS spectra and the results of their quantification for Ni-Re (1:1)/TiO$_2$ catalyst evidencing the formation of bimetallic Ni-Re nanoparticles and clusters.

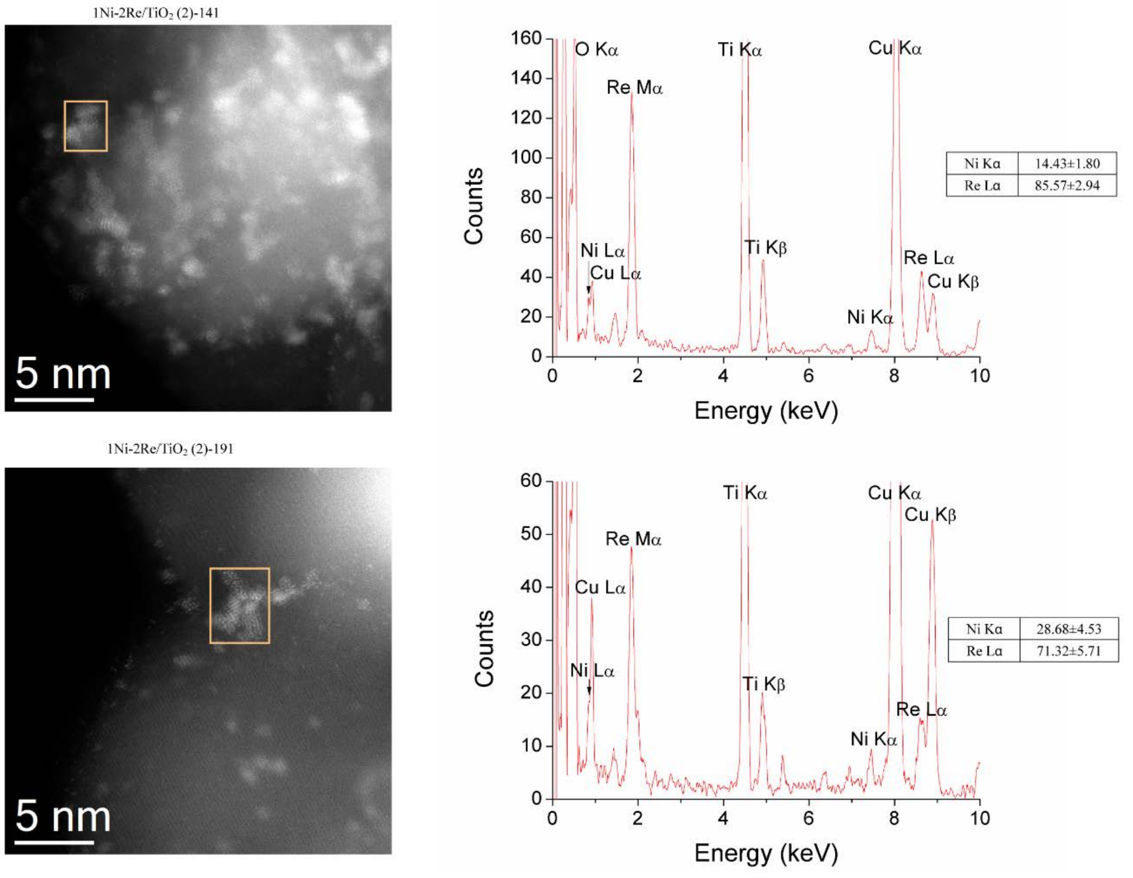

Figure S12. Representative STEM-HAADF micrographs together with the respective XEDS spectra and the results of their quantification for Ni-Re (1:2)/TiO_2 catalyst evidencing the formation of Ni-Re bimetallic nanoparticles.

N.B. The analysis of a large number of XEDS spectra collected at varied locations for different Ni-Re/TiO2 catalysts suggests a general trend for all materials that nanoparticles are more likely to be Re-rich, whereas sub-nanosized clusters are more Ni-rich or show chemical composition closer to the nominal metal loading ratio.

S2.4. Temperature-programmed reduction (TPR)

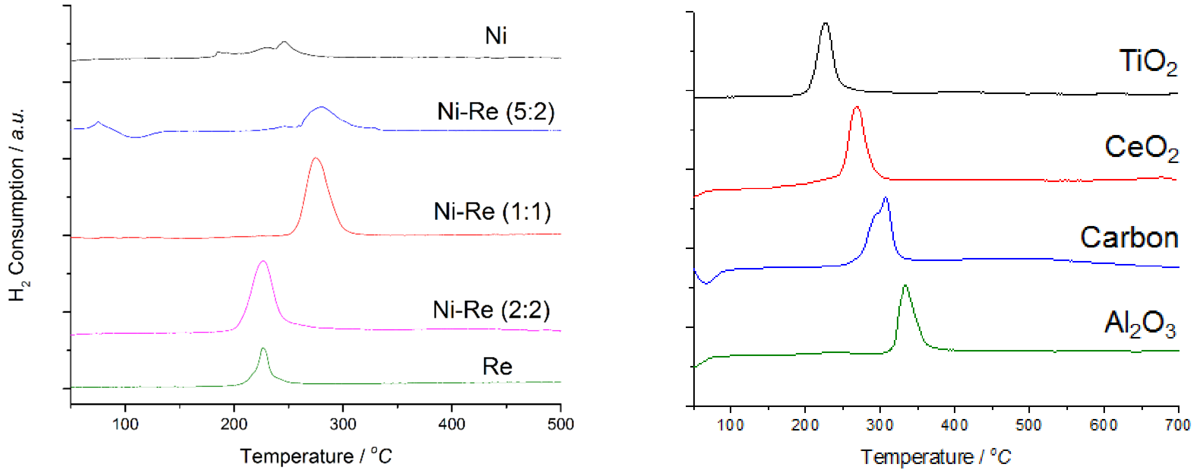

Figure S13 TPR profiles of (left) Ni-Re (*x*:*y*)/TiO_2 and (right) Ni-Re (1:2) on TiO_2, CeO_2, C and Al_2O_3 catalyst supports.

Table S1. Summary of calculated hydrogen-to-metal ratios for TiO_2-supported Ni, Re and Ni-Re (*x*:*y*)/TiO_2 catalysts.

	H_2/metal ratio
Ni (3 wt. %)/TiO_2	3.17
Ni:Re (1:1)/TiO_2	1.91
Ni:Re (1:2)/TiO_2	1.45
Ni:Re (2:1)/TiO_2	1.81
Ni:Re (5:1)/TiO_2	1.79
Re(13 wt. %)/TiO_2	2.17
Re (18 wt. %)/TiO_2	2.88

S2.5. X-ray photoelectron spectroscopy (XPS)

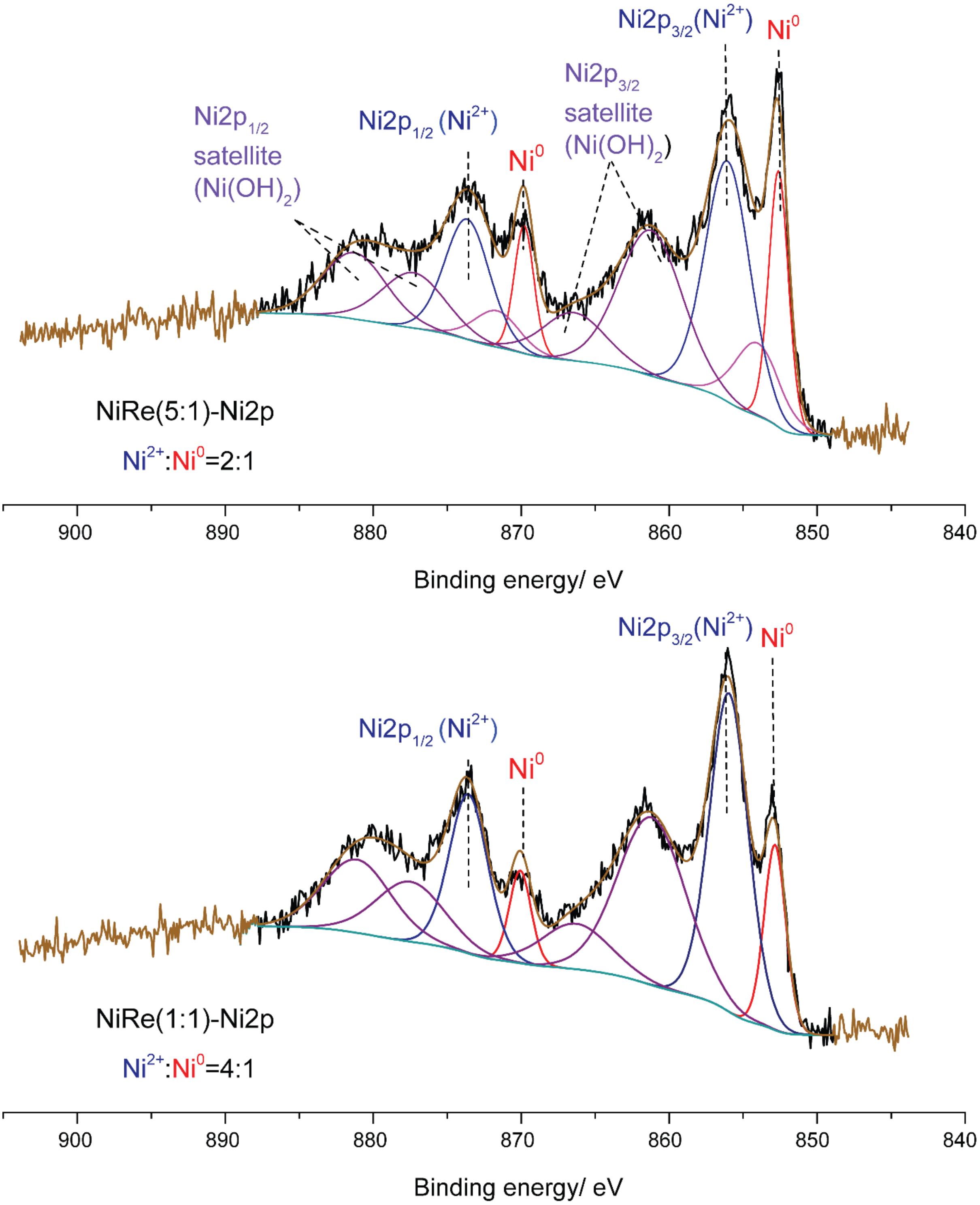

Figure S14 XP spectra of Ni(2p) region for the reduced Ni-Re (5:1) and Ni-Re(1:1)/TiO_2 catalyst.

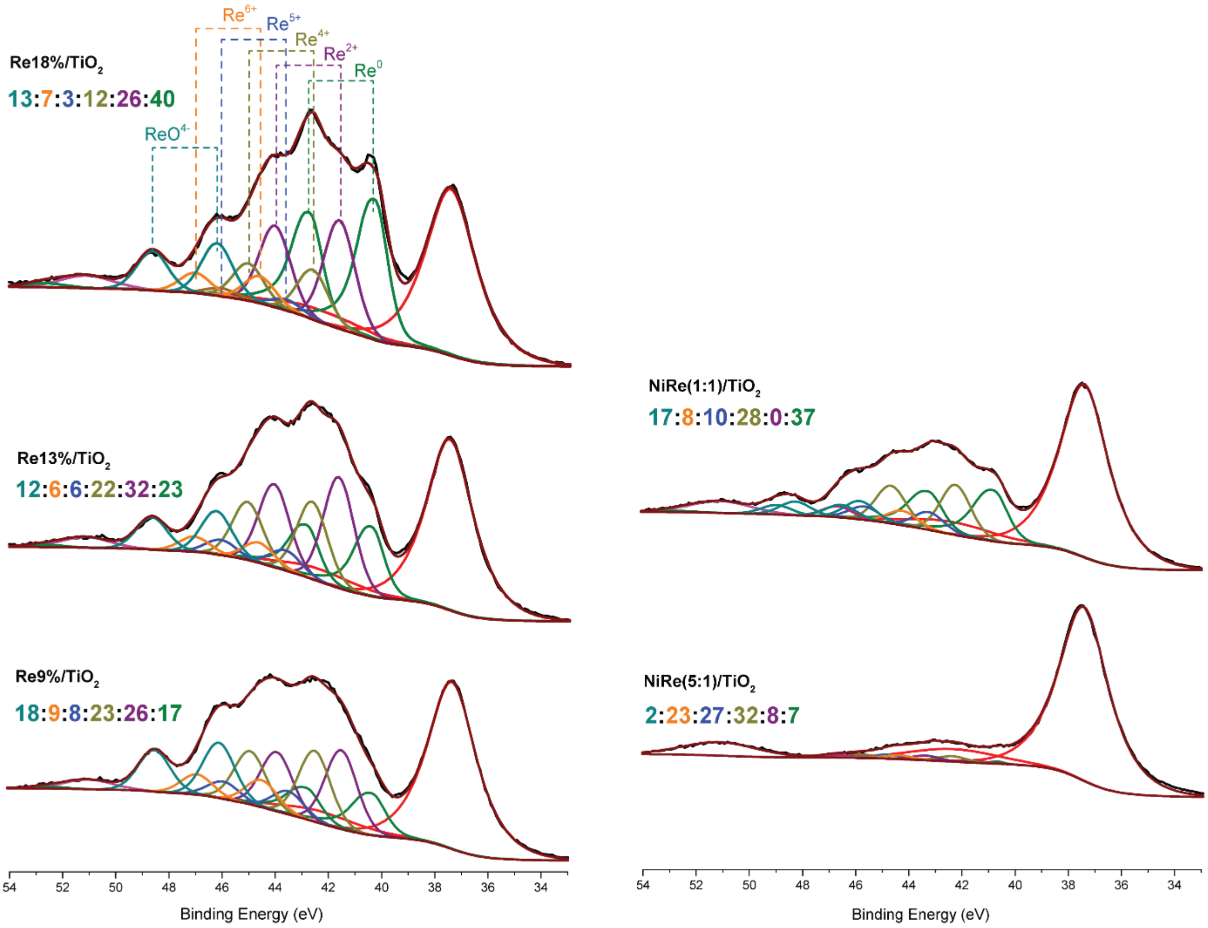

Figure S15. XP spectra in Re(4f) region of the reduced titania-supported Re- and Ni-Re catalysts.

S2.6. Supplementary activity measurements

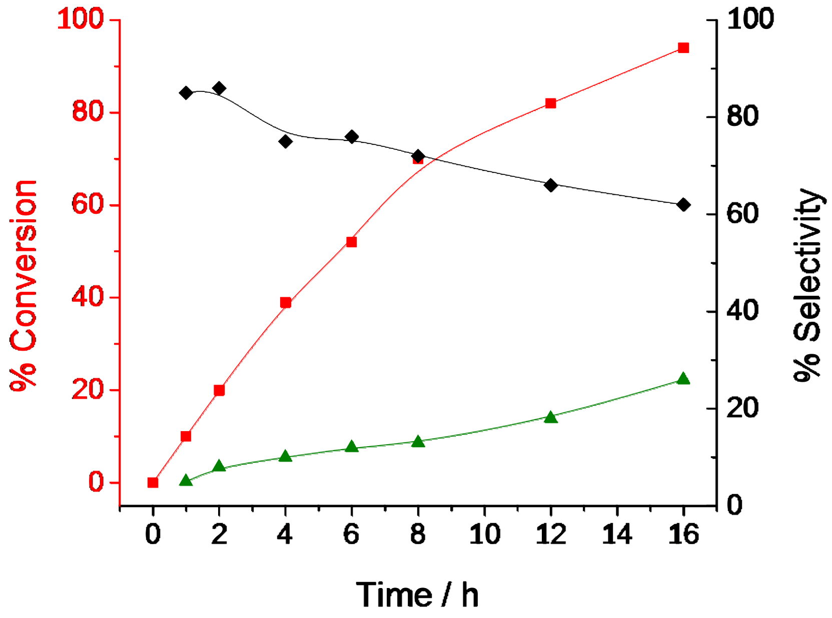

Figure S16 Time-on-line analysis for Ni-Re (1:2)/TiO_2 catalysts in the hydrogenation of methyl hexanoate in octane showing selectivity to 1-hexanol (black) and hexane (green). *Conditions:* Catalyst (18 mg), methyl hexanoate (0.44 mmol), hexane (3.5 mL), dodecane (35.2 µL), 180 °C, 50 bar H_2, 8 h, 1000 rpm.

Table S2 Evaluation of the activity of the TiO_2-supported Re catalysts in hydrogenation of methyl hexanoate in octane solvent. Catalyst (18 mg), methyl hexanoate (0.44 mmol), octane (3.5 mL), dodecane (35.2 µL), 180 °C, 50 bar H_2, 8 h, 1000 rpm.

Catalyst	**Conv. (%)**	**Selectivity to, %**		
		hexanol	**hexane**	**other**
Re (5%) /TiO_2	31	42	36	32
Re (13%) /TiO_2	70	75	7	18
Re (18%) /TiO_2	65	80	6	14

S2.7. Supplementary bright-field TEM catalyst characterization

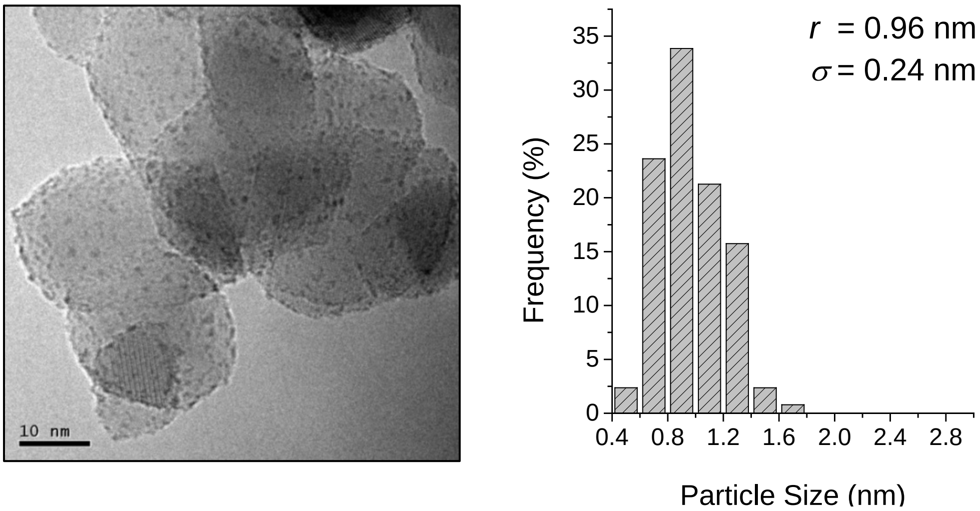

Figure S17 Representative TEM micrograph and corresponding particle-size distribution histogram for a Ni-Re(1:2)/TiO_2 catalyst recovered after methyl hexanoate hydrogenation reaction and re-reduced in 10% H_2 (300 °C/ 1 h).

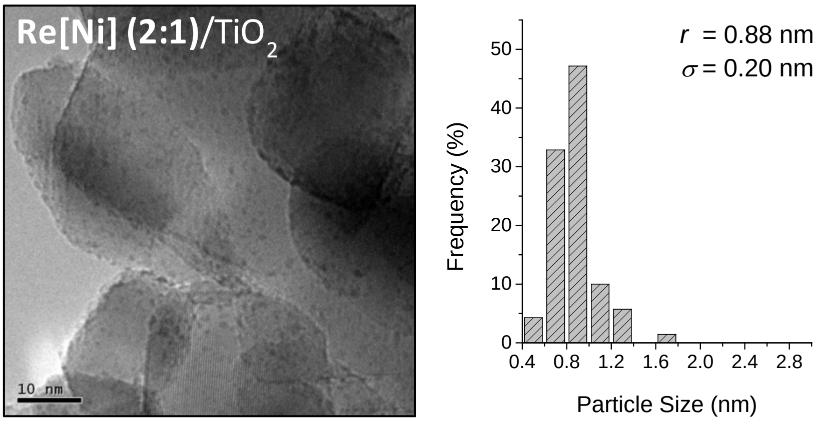

Figure S18 Representative TEM micrograph and corresponding particle-size distribution histogram for a Ni-Re(1:2)/TiO_2 catalyst prepared by a consecutive impregnation methodology and reduced twice in 10% H_2 (300 °C/ 2 h).